photonics

MDPI

Communication

Q-Switched Pulse Generation in a Multicore Fiber Laser with a Femtosecond-Laser-Inscribed FBG Array

Alexey G. Kuznetsov [1,*], Alexander V. Dostovalov [1,2] and Sergey A. Babin [1,2]

[1] Institute of Automation and Electrometry, 1 Ac. Koptyug Ave., Novosibirsk 630090, Russia; dostovalov@iae.nsk.su (A.V.D.); babin@iae.nsk.su (S.A.B.)
[2] Department of Physics, Novosibirsk State University, 2 Pirogov Str., Novosibirsk 630090, Russia
* Correspondence: kuznetsovag@iae.nsk.su

Abstract

A Q-switched pulsed laser based on a coupled 7-core Yb-doped fiber with a cavity based on a fiber Bragg grating array has been demonstrated with a maximum energy of microsecond pulses up to 15 μJ at a 1 kHz repetition rate. The lasing spectrum is hybridized so that the laser line maxima of each core are nearly the same, having a negligible spread relative to each other, which is much lower than the wavelength shifts between individual FBGs in the cores. At the same time, the generated power is nearly the same in all the cores. However, when increasing the power beyond the stimulated Raman scattering threshold, the supermodes are destroyed so that the spectra in the cores become increasingly different and less stable, and the output power is mainly concentrated in one of the cores, whereas the pulse shortens significantly to a sub-microsecond duration (300 ns), with damped oscillations appearing at the beginning. The new regimes we demonstrated of the multicore fiber laser are promising for creating powerful pulsed radiation sources with a narrow spectrum.

Keywords: fs laser inscription; multicore fiber; Raman scattering; Q-switch; LD pumping; beam shape

1. Introduction

Multicore fibers (MCFs) have recently attracted considerable interest as promising light guides for applications in communication [1,2], sensor [3,4] and laser technologies [5,6]. Communication and sensor applications typically require fibers with low core coupling to avoid distortions in the transmission of data and measured values. At the same time, lasers based on such fibers essentially represent multiple light sources from multiple cores but within a single fiber. Although this allows for minimizing the device size, beam combining must be performed at the output of the MCF cable, which requires a complex optical system to coherently combine all beams into a single beam with good quality [5].

As the distance between cores is reduced, strong optical coupling between them arises, forming supermodes (SMs) with fixed phases of the core modes. In this case, the emissions in a multicore fiber can be viewed not as a set of independent light sources but as a unified system. It is also possible to excite a single supermode with optimal characteristics for the power scaling of short pulses; for example, an out-of-phase SM in a square 5 × 5 MCF [6], which is shown to be resistant to discrete modulation instability, can carry a total peak power that greatly exceeds the self-focusing threshold for a single-core fiber.

The first continuous-wave (CW) MCF laser in an all-fiber configuration was proposed by Li et al. [7]. This laser was implemented in a 19-core Er/Yb codoped fiber in a configuration that allowed for the selection of the in-phase SM via the Talbot effect. Experiments

Check for updates

Received: 29 May 2026
Revised: 18 June 2026
Accepted: 24 June 2026
Published: 25 June 2026

Copyright: © 2026 by the authors. Licensee MDPI, Basel, Switzerland. This article is an open access article distributed under the terms and conditions of the Creative Commons Attribution (CC BY) license.

involving a single-mode fiber Bragg grating (FBG) attached to one core of a 4-core Yb-doped fiber [8] have demonstrated that the laser emits at the same wavelength in all cores matching the FBG reflection peak and thus ensuring that adequate coupling between the cores is achieved through the bending of the MCF. In [9], the effect of hybridization and spectral collapse was first demonstrated in a CW 7-core Yb-doped fiber laser with a femtosecond-laser-inscribed array of FBGs with individual characteristics, in contrast to simultaneous fabrication in MCFs of similar FBGs by the phase-mask technique [10]. It was shown that in the presence of optical coupling between the cores, the laser power is distributed uniformly across the cores, and the same narrowband spectrum is generated in all cores, despite the sufficient difference in individual FBG reflection spectra (both central wavelengths and shapes) [9].

Some studies have also been conducted on the pulsed operation of multicore fiber lasers with optically coupled cores, albeit most of the modern pulsed systems explore MCF amplifiers using a single-beam seed divided among independent amplifying cores and a subsequent combination of output beams with active control of their phases [5]. In MCF lasers, Q-switched pulsed regimes have been demonstrated by adding modulators to mode-selective MCF resonators, achieving mJ pulse energies with pulse durations in the 10 to 200 ns range. For example, a Q-switched laser based on a 6-core Yb-doped photonic crystal fiber was investigated in [11,12]—the resonator of which was constructed using a highly reflective (HR) mirror and a 4% mirror on the other laser side. Since the fiber cores were not single-mode (few-mode), an aperture was used for filtering in the far-field zone to suppress higher-order modes. Pulses with energies exceeding 2 mJ and a duration of 30 ns were obtained; however, the papers do not provide data on the spectrum of the generated signal. A similar pulsed laser, but with multi-mode cores in a 6-core fiber, was also investigated in [13]. In this work, the resonator was also constructed using free-space mirrors, i.e., without spectral filtering. A pulse energy of ~1.6 mJ was obtained with a pulse duration of 200 ns and a beam quality of M^2~2. However, this work also did not pay any attention to the optical spectrum analysis.

Overall, a brief overview of the literature shows that there is an extremely limited number of publications investigating MCF lasers built using FBG arrays in individual cores. In this paper, we continue our investigation of the generation regimes of a 7-core Yb-doped fiber laser with a resonator based on an FBG array with wavelength-shifted FBGs. We have implemented a pulsed regime for such MCF lasers by means of active Q-switching using an acousto-optic modulator (AOM), thus generating pulses with a repetition rate of 1–50 kHz. Spatial, temporal and spectral characteristics of the laser radiation generated in the Q-switched MCF laser with a femtosecond-laser-inscribed FBG array have been studied, and next-generation regimes have been demonstrated for the first time, to our knowledge.

2. Materials and Methods

In the present work, we used a 7-core fiber manufactured at the Dianov Fiber Optic Research Center, Moscow, Russia, using the drilling method; see [10] for details. For the cores, the rods were obtained by drawing a single-core preform fabricated by depositing an Al_2O_3–GeO_2–SiO_2 matrix glass as a porous layer using a modified chemical vapor deposition (MCVD) method, followed by impregnation with an aqueous solution of $Yb(NO_3)_3$. The refractive index difference between the core and cladding was $\Delta n = 0.008$. The multicore optical fibers were coated with a reflective polymer, providing wave-guiding of multi-mode pump radiation. The absorption coefficient in each core was ~400 dB/m at a wavelength of 976 nm for a weak single-mode signal. The cores were arranged hexagonally with a spacing of 17.2 μm, while the cladding and core diameters were 135 and 4 μm,

respectively. Such an arrangement is characterized by sufficient optical coupling of the cores that was additionally enhanced by coiling the MCF with a diameter of 6 cm.

To fabricate fiber optic gratings, we used a direct point-by-point inscription method [14] with a Light Conversion Pharos-6W (Vilnius, Lithuania) ultrashort pulse laser (λ = 1026 nm, Δt = 232 fs, f = 1 kHz), and we achieved the fiber pulling by using an Aerotech ABL1000 (Pittsburgh, PA, USA) translation stage at a speed of 0.733 mm/s. The length of each FBG was 2 mm, with a period of 0.733 μm, corresponding to the second-order reflection at a wavelength of 1064 nm. All FBGs were aligned in the same longitudinal direction; the orientation of their grooves in the cross-section was azimuthal, with the exception of the central core, which had a radial groove. The full width at half maximum (FWHM) of the resonance peak (R > 90%) in the reflection spectra of each FBG was around 0.4 nm, whereas their central wavelengths were significantly shifted to each other (up to ~0.3 nm) with a rather narrow overlap (<0.2 nm) between the individual FBG reflection spectra (Figure 1).

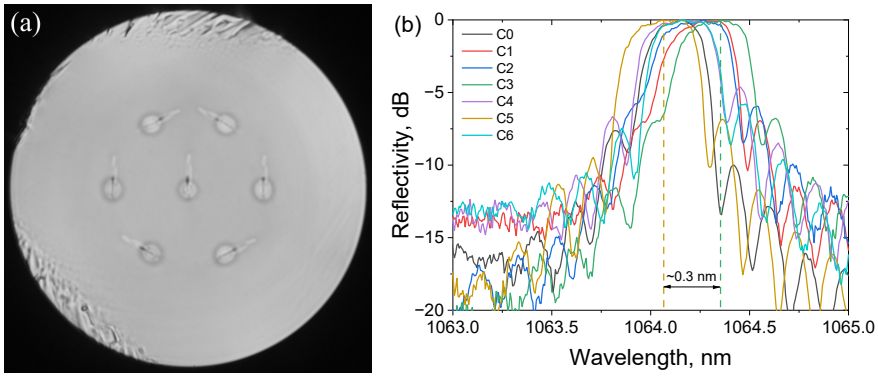


Figure 1. Fiber cross-section with fs-inscribed highly reflective (HR) FBGs (**a**) and individual FBG reflection spectra of the 7-core FBG array (C0-central, C1–C6 peripheral) (**b**).

Figure 2 shows the schematic of the studied Q-switched 7-core fiber laser. A fiber-pigtailed multi-mode laser diode (105/125 μm, NA 0.22) with a power of up to 25 W at a wavelength of 976 nm was used for pumping the MCF. The output end of the laser diode fiber was spliced directly to a 7-core active fiber with a light-guiding cladding. The length of the active fiber was ~30 m—on one end of which the HR FBG array was inscribed, and the other end was cleaved at an angle of ~10° to minimize the Fresnel reflection. The radiation emerging from the fiber was collimated by a lens with a focal length of f = 3 mm and directed into the input of a free-space acousto-optic modulator (AOM), model AA opto-electronic (Orsay, France) QS40-A1-L1064-z32, with a carrier frequency of 40.68 MHz. At the AOM output, the +1 diffraction order was reflected back into the laser using mirror M1 with a reflectivity of R~90%, thus providing feedback with minimal inter-pulse background. The light passing through M1 was additionally filtered by dichroic mirrors from unabsorbed pump radiation at 976 nm, was coupled to a 50/125 μm multi-mode fiber and was analyzed using a photodiode (1 GHz), an optical spectrum analyzer (OSA) and a profilometer. Rectangular electrical pulses with a duty cycle of ~6%, generated by a waveform generator, were applied to the AOM. Figure 2b shows an example of the generated trains of output laser pulses with a repetition rate of 1 kHz. To analyze the output radiation in the individual cores, an aperture was installed along the optical path, which was used to isolate the corresponding beam.

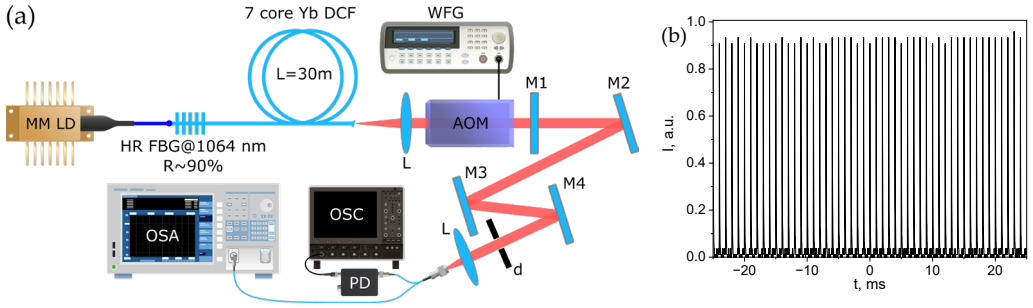


Figure 2. (**a**) Scheme of a Yb-doped multicore fiber pulsed laser: MM LD—multi-mode laser diode; HR FBG—fs-inscribed high-reflective FBG; L—collimating lens; M1—90% reflecting mirror, M2–M3—dichroic mirrors; OSA—optical spectrum analyzer; OSC—oscilloscope; PD—photodiode module; AOM—acousto-optic modulator; WFG—waveform generator; d—diaphragm. (**b**) Output pulse train at an LD pump power of 1.4 W and repetition rate of 1 kHz.

3. Results

The pulsed generation threshold in the laser under study was ~1.1 W of the laser diode pumping at a pulse repetition rate of 1 kHz, and stable pulse trains were formed at a pump power of 1.4 W (Figure 2b). Figure 3b shows the pulse shapes in each core at a pump power of 1.4 W; the durations of which are approximately 3.5 µs. The total average output power from all cores was 10 mW, which is equivalent to 2.9 W of the peak power for this pulse shape. Thus, the peak output power from each core is approximately 0.41 W. Figure 3b shows the corresponding optical spectra of individual cores, from which it is evident that all the generation spectra have nearly the same maximum at ~1064.3 nm, whereas the spectral widths (FWHM) slightly vary within the range of 0.16–0.22 nm. It is noteworthy that the spread of the lasing lines is significantly smaller than the spread of the maxima of corresponding individual FBG reflection spectra (see Figure 1). This spectral collapse effect has already been observed in the case of a continuous-wave 7-core fiber laser [9], but the individual lasing spectra in the cores were significantly narrower in the CW regime.

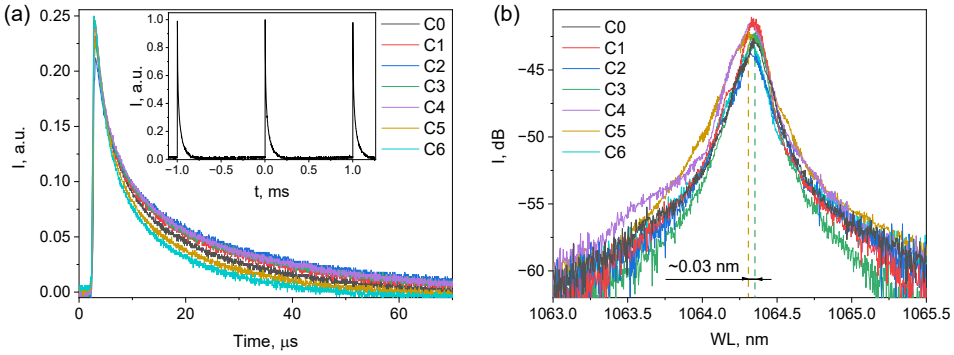


Figure 3. Output laser pulse shapes (**a**) and optical spectra (**b**) in individual cores at a pump power of 1.4 W, with a rep. rate of 1 kHz.

Increasing the pump power to 1.7 W results in a sharp narrowing of the pulse duration (Figure 4a), but the temporal stability deteriorates, a jitter of ~0.5 µs appears, and the pulse amplitude (peak-to-peak) can vary by 40%, as can be seen in the inset of Figure 4a. In this case, a narrowband sub-microsecond (~300 ns FWHM) pulse train is generated, and the peak power reaches ~50 W, which is equivalent to ~7 W/core. The generated spectrum also becomes less stable, and the individual core lines differ more significantly (Figure 4b). Figure 5 compares the lasing spectra over a wide wavelength range for the cases with a pump power of 1.4 W and 1.7 W and in a continuous mode (also with a pump power of 1.7 W). It can be seen that in the pulsed mode with a pump power of 1.7 W, the spectrum

contains, in addition to the main 1064 nm signal, stimulated Raman scattering (SRS) with a large number of higher Stokes orders spanning from 1100 nm up to 1350 nm. Using a fiber thin-film filter, we isolated the spectral range > 1100 nm and analyzed the temporal dynamics, which are shown in Figure 5b. The SRS pulse exhibits initial oscillations lasting up to 10 ns, which gradually decay, and the FWHM of the pulse extends to 130 ns.

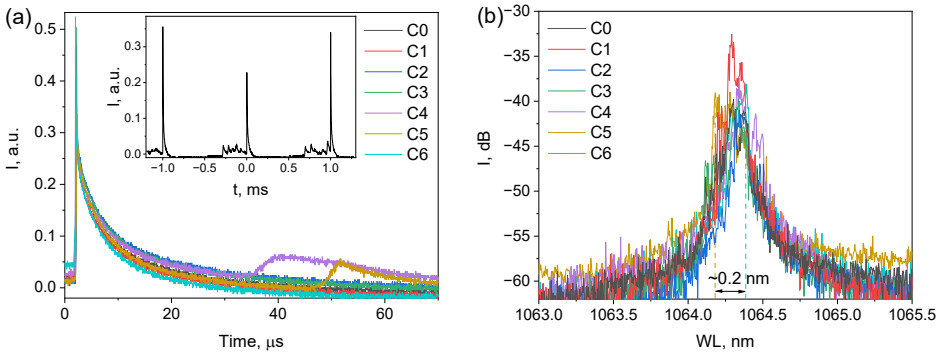


Figure 4. Output laser pulses (**a**) and optical spectra (**b**) at pump power of 1.7 W and rep. rate of 1 kHz.

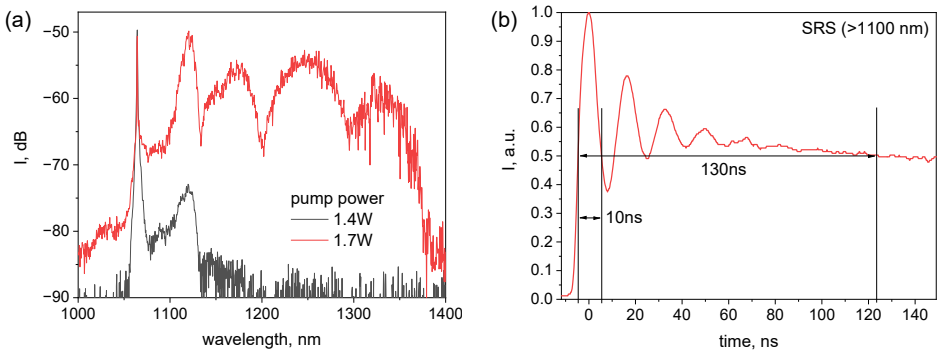


Figure 5. Output optical spectra at different powers (**a**) and the SRS pulse component at pump power of 1.7 W (**b**).

The power distribution across the cores was also measured over time, as shown in Figure 6. Here, a difference is also observed for cases below and above the SRS threshold. At a pump power of 1.4 W, the generated power is distributed relatively uniformly across the cores and varies little over time. When SRS arises, a significant portion of the total power (the useful signal at a wavelength of 1064 and the SRS components) becomes concentrated in core #4. We also filtered the 1064 nm signal with an interference filter and obtained a virtually identical intensity distribution; i.e., the transfer to the selected core occurs for all components of the generated spectrum. Furthermore, fairly strong pulsations occur over time, which contrasts with the previous case.

We also tested the possibility of increasing the repetition rate to 50 kHz (Figure 7). In this case, to maintain stable pulses, it was necessary to increase the pump power to 28 W, while the pulse duration was 3.8 μs, and the average power was 1.1 W, which corresponds to 5.8 W of the peak power. Since the pulses have a long falling tail, a further increase in the pulse repetition rate is accompanied by an increase in the offset, when the previous pulse does not have time to completely fall to zero, and a new pulse begins to form against it.

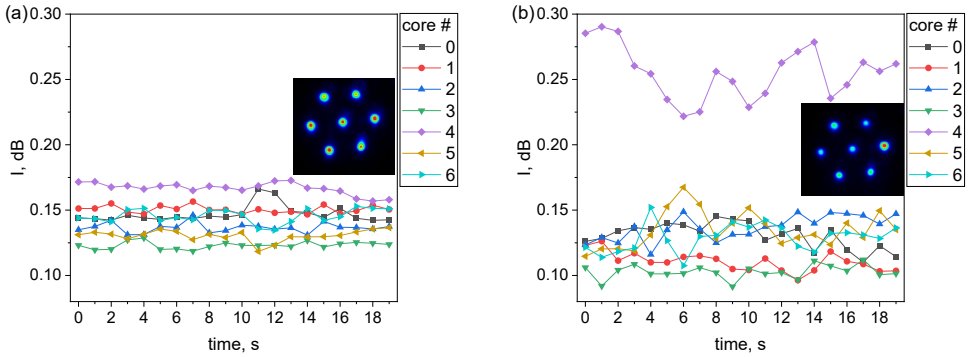


Figure 6. Dynamics of power distribution across the cores at 1.4 W (**a**) and 1.7 W (**b**) pumping.

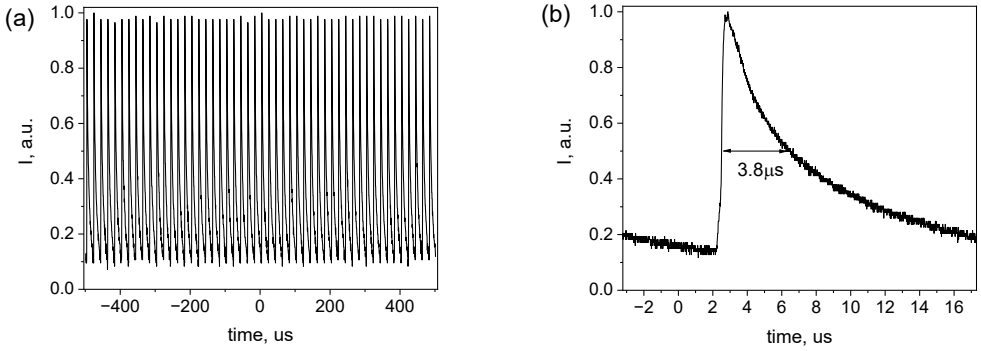


Figure 7. Train of pulses at a repetition frequency of 50 kHz (**a**) and corresponding optical pulse shape (**b**).

4. Discussion and Conclusions

Thus, a Q-switched pulsed fiber laser based on a 7-core Yb fiber was demonstrated. The key element of the laser is an FBG array recorded in each individual core with a wavelength spread of reflection maxima of approximately 0.3 nm. With a pump power of 1.4 W and a specified AOM repetition rate of 1 kHz, pulses of 3.5 μs durations with a total peak power of 2.9 W are formed. The lasing spectrum in this regime is hybridized, so that the lasing line maxima of each core has a negligible spread relative to each other (~0.03 nm), which is an order of magnitude smaller than the spread of the FBG reflection maxima. The spectral collapse effect has already been observed by us in a continuous-wave all-fiber laser [9], in which the output mirror was a straight cleave of the fiber with a 4% Fresnel reflection back into the fiber. Now, it has been shown that this effect also occurs with a free-space mirror and in the Q-switched pulsed generation regime.

At the same time, as the pump power increases and the SRS generation threshold is exceeded, the output pulse shortens significantly to a sub-microsecond duration (300 ns), with damped oscillations appearing at the beginning of the pulse, whereas the peak power and pulse energy reach 50 W and 15 μJ respectively. The output signal spectrum of each core exhibits noisy peaks near 1064 nm, with a spread increasing to ~0.2 nm. It can be assumed that core de-synchronization occurs, and supermodes are destroyed in this regime. Thus, the laser operation approaches a laser without intercore coupling (see [9]), which was achieved by significantly increasing the distance between the cores in [9]. Here, a strong Raman conversion of the generated pulses arises, which also influences the output characteristics.

The spatial distribution of the output signal power differs significantly for the two obtained generation regimes. At a pump power of 1.4 W, the power distribution across the cores differs only slightly and is quite stable over time. In contrast, when the Raman threshold is exceeded, a strong skew in energy distribution occurs, and the brightest core is

favored, while the remaining cores divide the remaining energy almost evenly. At the same time, this leads to strong random power fluctuations in the cores. It can be assumed that, since supermodes are destroyed, lasing in the cores occurs more independently; meaning that the cores with lower losses (during coil twisting, during the return from the mirror to the fiber through an oblique cleavage, etc.) are favored. A similar effect was observed with the strong coiling of the 4-core Yb-doped MCF with the FBG resonator [15], but here an additional role of the Raman process also seems important. It may induce nonlinear losses that are different for different cores.

Thus, at the transition from the CW to Q-switched regime in a coupled multicore fiber with an FBG array, the effect of the spectrum hybridization is preserved when the generation in individual cores has a common maximum in spite of different FBG wavelengths and the envelope of the total generation spectrum is significantly narrowed in comparison with the case of uncoupled cores where generation spectra mimic individual FBG spectra. This so-called collapse effect is defined by supermode formation and hybridization due to the core coupling. With the increasing pump power (and a peak power of 50 W that is beyond the SRS threshold), the effect of the supermode destruction on the Q-switched laser spectral and spatial characteristics of the output radiation is clearly demonstrated. It should be noted that the presented laser design's parameters were far from optimal. For example, we used an excessively reflecting output mirror, which reduced the output power and simultaneously led to the accumulation of high intracavity energy. In addition, the relatively long cavity affects the pulse duration, and the large-diameter output beam resulted in an increased response time in the AOM, which also delays the pulse leading edge. The further optimization of the laser scheme, including shortening the resonator and replacing the output mirror with a less reflective one, will help to reduce the pulse duration and its long falling edge, as well as increase the output power, including by means of shifting the intracavity SRS threshold.

Multicore fiber Q-switched lasers have been studied previously, but most of these lasers utilize bulk mirrors that reflect beams from all cores. For example, in [12] a resonator was formed by a highly reflective mirror and a Fresnel reflection from the output end. In [16] authors used two mirrors with reflectivities of 4% and 40%, respectively. Such designs are simple to implement, but they sacrifice the significant potential of multicore resonators and the flexibility to implement next-generation modes. Unlike previously published studies, we propose a resonator based on an array of reflectors for each core. This approach has already demonstrated new effects in continuous lasers, such as spectrum collapse due to supermode formation, and has now been tested in a pulsed Q-switched laser, in which additional effects associated with SRS have emerged, imposing some restrictions on the maximum output power during stable generation as well as new opportunities for laser pulse shortening and conversion to Stokes-shifted wavelengths in a broad spectral range.

A similar approach to pulse formation in a multi-mode fiber was implemented in [17]. The authors used an AOM to modulate the Q-factor of a Raman laser cavity with a frequency close to the cavity roundtrip time and thus obtained multicomponent pulses of the first and second Stokes orders of SRS in the output radiation. The appearance of the second-order Stokes radiation was accompanied by the modulation of the first-order Stokes pulse shape and the formation of a multipulse comb, vaguely reminiscent of the pulse oscillations we obtained here at 1.7 W pumping.

In conclusion, the technology under study of multicore lasers with an FBG array is of interest for future promising work aimed at creating powerful stable radiation sources (both pulsed and continuous) with a narrow spectrum. This laser can be further used in the microprocessing of materials as well as in sensor systems, LIDAR, etc.

Author Contributions: Conceptualization, S.A.B., A.G.K. and A.V.D.; methodology, A.G.K.; validation A.G.K., investigation, A.G.K. and A.V.D.; writing—original draft preparation, A.G.K.; writing—review and editing, S.A.B.; supervision and funding acquisition, S.A.B. All authors have read and agreed to the published version of the manuscript.

Funding: This research was funded by Russian Science Foundation (grant number 21-72-30024-П).

Data Availability Statement: Data are available upon request.

Acknowledgments: This work was carried out using the equipment of the Center for Collective Use "Spectroscopy and Optics" of the IAE SB RAS.

Conflicts of Interest: The authors declare no conflicts of interest.

References

1. Saitoh, K.; Matsuo, S. Multicore fiber technology. *J. Light. Technol.* **2016**, *34*, 55–66.
2. Melo, C.; Reyes, F.M.; Arroyo, D.; Gómez, E.S.; Walborn, S.P.; Lima, G.; Figueroa, M.; Cariñe, J.; Saavedra, G. All-fiber architecture for high speed core-selective switch for multicore fibers. *Commun. Eng.* **2025**, *4*, 77. [PubMed]
3. Wang, S.; Zhang, W.; Chen, L.; Zhang, Y.; Geng, P.; Wang, B.; Yan, T.; Li, Y.; Hu, W. Bending Vector Sensor Based on the Multimode-2-Core-Multimode Fiber Structure. *IEEE Photonics Technol. Lett.* **2016**, *28*, 2066–2069.
4. Yao, Y.; Zhao, Z.; Tang, M. Advances in multicore fiber interferometric sensors. *Sensors* **2023**, *23*, 3436. [CrossRef] [PubMed]
5. Klenke, A.; Jauregui, C.; Steinkopff, A.; Aleshire, C.; Limpert, J. High-power multicore fiber laser systems. *Prog. Quant. Electron.* **2022**, *84*, 100412. [CrossRef]
6. Kalinin, N.A.; Anashkina, E.A.; Egorova, O.N.; Zhuravlev, S.G.; Semjonov, S.L.; Kim, A.V.; Litvak, A.G.; Andrianov, A.V. Controlled Excitation of Supermodes in a Multicore Fiber with a 5 × 5 Square Array of Strongly Coupled Cores. *Photonics* **2021**, *8*, 314. [CrossRef]
7. Li, L.; Schulzgen, A.; Li, H.; Temyanko, V.L.; Moloney, J.V.; Peyghambarian, N. Phase-locked multicore all-fiber lasers: Modeling and experimental investigation. *J. Opt. Soc. Am. B* **2007**, *24*, 1721–1728.
8. Kurkov, A.S.; Babin, S.A.; Lobach, I.A.; Kablukov, S.I. Mechanism of mode coupling in multicore fiber lasers. *Opt. Lett.* **2008**, *33*, 61–63. [PubMed]
9. Kuznetsov, A.G.; Wolf, A.A.; Egorova, O.N.; Semjonov, S.L.; Dostovalov, A.V.; Podivilov, E.V.; Babin, S.A. Spectrum collapse in a 7-core Yb-doped fiber laser with an array of fs-inscribed fiber Bragg gratings. *Opt. Lett.* **2023**, *48*, 3603–3606. [PubMed]
10. Alon, Y.; Halstuch, A.; Sidharthan, R.; Yoo, S.; Ishaaya, A.A. Femtosecond Bragg grating inscription in an Yb-doped large-mode-area multicore fiber for high-power laser applications. *Opt. Lett.* **2020**, *45*, 4563–4566. [PubMed]
11. Michaille, L.; Bennett, C.R.; Taylor, D.M.; Shepherd, T.J. Multicore photonic crystal fiber lasers for high power/energy applications. *IEEE J. Sel. Top. Quant. Electron.* **2009**, *15*, 328–336. [CrossRef]
12. Michaille, L.; Taylor, D.M.; Bennett, C.R.; Shepherd, T.J.; Ward, B.G. Characteristics of a Q-switched multicore photonic crystal fiber laser with a very large mode field area. *Opt. Lett.* **2008**, *33*, 71. [PubMed]
13. Benudiz, Y.; Raghuraman, S.; Zang, J.; Ami, B.U.; Yoo, S.; Ishaaya, A.A. 16 W large-mode-area multi-core Q-switched fiber laser. In *Proceedings of the Laser Congress 2019 (ASSL, LAC, LS&C), OSA Technical Digest, Vienna, Austria, 29 September–3 October 2019*; Optica Publishing Group: Washington, DC, USA, 2019; p. JTh3A.43.
14. Wolf, A.; Dostovalov, A.; Bronnikov, K.; Skvortsov, M.; Wabnitz, S.; Babin, S. Advances in femtosecond laser direct writing of fiber Bragg gratings in multicore fibers: Technology, sensor and laser applications. *Opto-Electron. Adv.* **2022**, *5*, 210055. [CrossRef]
15. Wolf, A.A.; Skvortsov, M.I.; Lobach, I.A.; Dostovalov, A.V.; Babin, S.A. Bending induced output power concentration in a core of a 4-core Yb-doped fiber laser. *Opt. Express* **2022**, *30*, 7580–7590. [CrossRef] [PubMed]
16. Nassiri, A.; Idrissi-Saba, H.; Boulezhar, A. Analysis of Ytterbium Doped Seven-core Fiber Laser for MaterialsProcessing and Particle Image Velocimetry Applications. In *Proceedings of the 1st International Conference of Computer Science and Renewable Energies*; SciTePress: Setúbal, Portugal, 2020; pp. 260–263.
17. Kuznetsov, A.G.; Kablukov, S.I.; Timirtdinov, Y.A.; Babin, S.A. Actively Mode Locked Raman Fiber Laser with Multimode LD Pumping. *Photonics* **2022**, *9*, 539. [CrossRef]

Disclaimer/Publisher's Note: The statements, opinions and data contained in all publications are solely those of the individual author(s) and contributor(s) and not of MDPI and/or the editor(s). MDPI and/or the editor(s) disclaim responsibility for any injury to people or property resulting from any ideas, methods, instructions or products referred to in the content.